Ribosomal binding to the internal ribosomal entry site of classical swine fever virus

V. G. Kolupaeva, T. V. Pestova and C. U. Hellen

RNA 2000 6: 1791-1807

RNA (2000), *6*:1791–1807. Cambridge University Press. Printed in the USA.

Ribosomal binding to the internal ribosomal entry site of classical swine fever virus

VICTORIA G. KOLUPAEVA,[1] TATYANA V. PESTOVA,[1,2] and CHRISTOPHER U.T. HELLEN[1]

[1]Department of Microbiology and Immunology, State University of New York Health Science Center at Brooklyn, Brooklyn, New York 11203, USA
[2]A.N. Belozersky Institute of Physico-Chemical Biology, Moscow State University, 119899 Moscow, Russia

ABSTRACT

Most eukaryotic mRNAs require the cap-binding complex eIF4F for efficient initiation of translation, which occurs as a result of ribosomal scanning from the capped 5′ end of the mRNA to the initiation codon. A few cellular and viral mRNAs are translated by a cap and end-independent mechanism known as internal ribosomal entry. The internal ribosome entry site (IRES) of classical swine fever virus (CSFV) is ~330 nt long, highly structured, and mediates internal initiation of translation with no requirement for eIF4F by recruiting a ribosomal 43S preinitiation complex directly to the initiation codon. The key interaction in this process is the direct binding of ribosomal 40S subunits to the IRES to form a stable binary complex in which the initiation codon is positioned precisely in the ribosomal P site. Here, we report the results of analyses done using enzymatic footprinting and mutagenesis of the IRES to identify structural components in it responsible for precise binding of the ribosome. Residues flanking the initiation codon and extending from nt 363–391, a distance equivalent to the length of the 40S subunit mRNA-binding cleft, were strongly protected from RNase cleavage, as were nucleotides in the adjacent pseudoknot and in the more distal subdomain $IIId_1$. Ribosomal binding and IRES-mediated initiation were abrogated by disruption of helix 1b of the pseudoknot and very severely reduced by mutation of the protected residues in $IIId_1$ and by disruption of domain IIIa. These observations are consistent with a model for IRES function in which binding of the region flanking the initiation codon to the decoding region of the ribosome is determined by multiple additional interactions between the 40S subunit and the IRES.

Keywords: classical swine fever virus; eIF3; enzymatic footprinting; initiation; internal ribosomal entry site; ribosome; translation

INTRODUCTION

Initiation of protein synthesis requires the coordinated action of multiple translation components to mediate assembly of an 80S ribosome at the initiation codon of an mRNA (Merrick, 1992). First, a 43S complex is assembled from aminoacylated initiator tRNA, eukaryotic initiation factors (eIFs) 2 and 3, GTP and the small (40S) ribosomal subunit. On the majority of mRNAs, eIF4F binds to the 5′-terminal cap and promotes binding of the 43S complex to a cap-proximal region of the mRNA. This complex requires eIFs 1 and 1A to locate the initiation codon by scanning in a 5′-3′ direction (Pestova et al., 1998a). The resulting 48S complex is joined at the initiation codon by a large ribosomal subunit to form an 80S ribosome that is competent to begin protein synthesis (Pestova et al., 2000). The accuracy of initiation codon selection is thought to be ensured by the base-by-base inspection of the 5′ nontranslated region (5′ NTR) by the scanning ribosome, which continues until base pairing is established between the initiation codon and the anticodon of initiator tRNA.

Translation initiation on various eukaryotic cellular and viral mRNAs is 5′-end independent, and on a growing number of these mRNAs is known to occur following ribosomal attachment to an internal ribosomal entry site (IRES) (Johannes & Sarnow, 1998; Johannes et al., 1999). IRESs are complex RNA structures that may contain multiple AUG triplets upstream of the initiation codon that are not recognized as start sites for translation (e.g., Reynolds et al., 1996; Pelletier et al., 1988). Initiation codon selection therefore occurs by a mechanism unrelated to scanning. One well-characterized group of IRESs includes hepatitis C virus (HCV) and classical swine fever virus (CSFV) (Tsukiyama-Kohara et al.,1992; Rijnbrand et al., 1997). These IRESs are

Reprint requests to: Christopher U.T. Hellen, Department of Microbiology and Immunology, State University of New York Health Science Center at Brooklyn, 450 Clarkson Avenue, Box 44, Brooklyn, New York 11203, USA; e-mail: chellen@netmail.hscbklyn.edu.

~330 nt long (Fig. 1), and comprise most of the 5′ NTR (structural domains II and III, and a complex pseudoknot upstream of the initiation codon) and ~30 nt of the adjacent coding sequence (Reynolds et al., 1995; Lemon & Honda, 1997; Hellen & Pestova, 1999). They have related structures even though their sequences differ by ~55% (Wang et al., 1995; Le et al., 1998). These IRESs promote ribosomal attachment ("entry") at the initiation codon without prior scanning (Reynolds et al., 1996; Rijnbrand et al., 1996, 1997).

The mechanism of initiation on these IRESs has been investigated by mutational analysis and by reconstituting the initiation process in vitro using purified translation components to identify which factors are required for this process and to characterize their functions during it (Pestova et al., 1998b; Pestova & Hellen, 1999). These IRESs use an initiation mechanism that differs fundamentally from cap-mediated ribosomal scanning. The first stage is exceptionally simple: 43S complexes bind directly to these IRESs independently of eIFs 1,

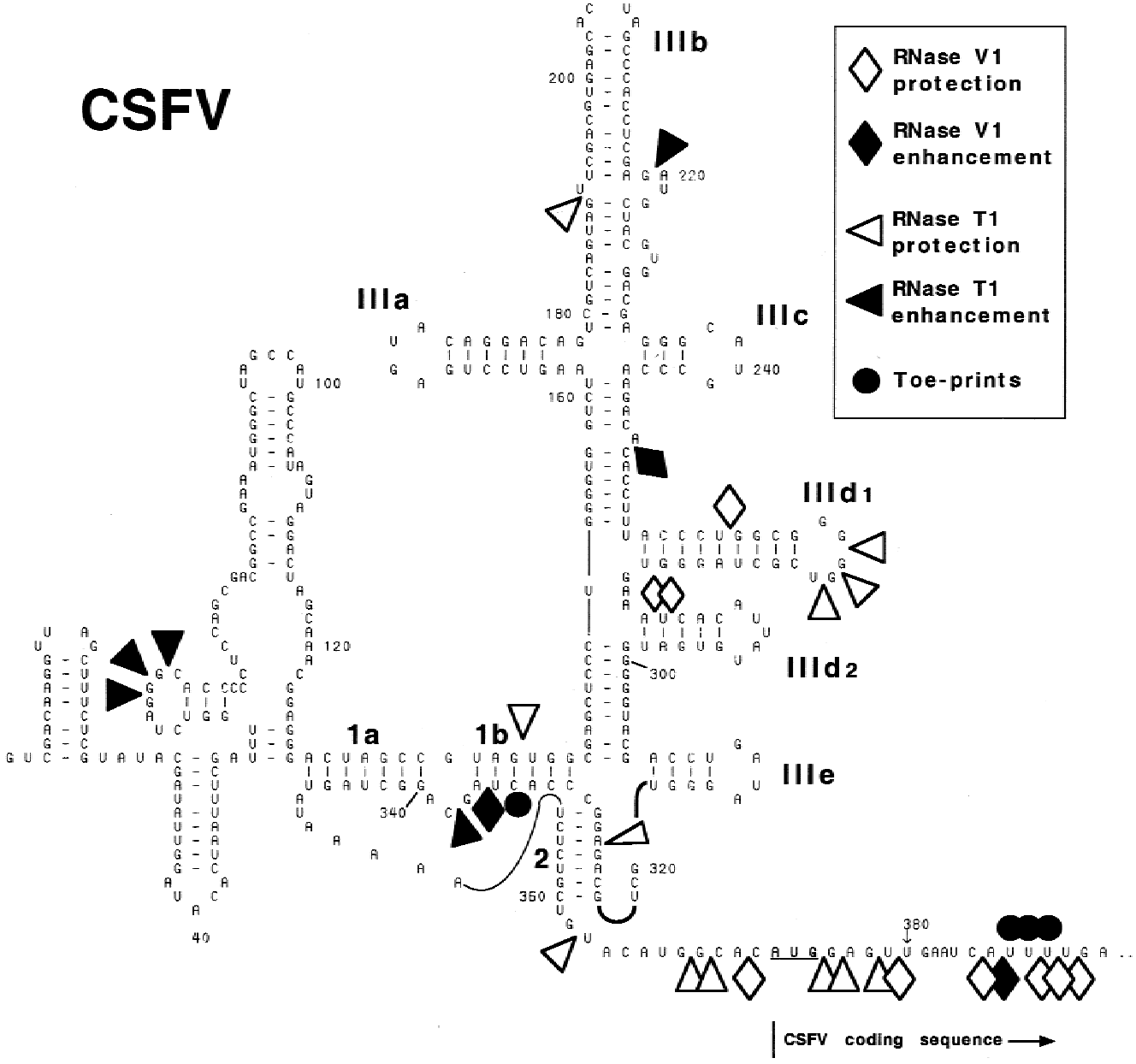

FIGURE 1. Schematic representation of the secondary structure of the CSFV IRES (based on Brown et al., 1992; Wang et al., 1995; Sizova et al., 1998) showing sites that are either protected from cleavage by RNAses T_1 and V_1 or at which cleavage is enhanced following binding of a 40S ribosomal subunit. These sites and the position of toeprints caused by bound 40S subunits are indicated by symbols tabulated at the upper right. The initiation codon ($AUG_{373–375}$) is underlined. IRES subdomains are named using nomenclature proposed by Honda et al. (1996) for the HCV IRES. The helices that constitute the pseudoknot are labeled 1a, 1b, and 2.

1A, 4A, 4B, and 4F (Pestova et al., 1998a, 1998b). This binding step is very precise so that the initiation codon is positioned in the immediate vicinity of the ribosomal P site (Pestova et al., 1998b) and results from specific interactions between elements of the IRES and components of the 43S complex. Two such interactions have been identified in addition to codon–anticodon base pairing. The apical half of domain III is bound by eIF3 (Buratti et al., 1998; Pestova et al., 1998b; Sizova et al., 1998; Odreman-Macchioli et al., 2000). In addition, these IRESs contain as yet undefined determinants that mediate factor-independent binding of 40S subunits at the initiation codon (Pestova et al., 1998b; Pestova & Hellen, 1999). The ability to bind directly to the small ribosomal subunit is highly unusual among eukaryotic mRNAs and has, to date, been reported only for CSFV-like IRESs and, very recently, for the unrelated IRES in the intergenic region of Cricket paralysis virus (Wilson et al., 2000). Direct binding of small (30S) ribosomal subunits to mRNA through Shine–Dalgarno base pairing is characteristic of initiation in prokaryotes (Shine & Dalgarno, 1974). However, binding of eukaryotic 40S subunits to CSFV-like IRESs is stabilized by multiple IRES–40S subunit interactions and is thus not directly analogous to the prokaryotic interaction. For example, primer extension on the CSFV IRES is arrested by a bound 40S subunit at C_{334} in the pseudoknot and at $UUU_{387–389}$ downstream of the initiation codon. This observation suggests that the initiation codon and flanking residues are fixed in the mRNA-binding cleft of the 40S subunit, and that the 40S subunit binds the IRES at one or more additional positions.

We report here that we have identified nucleotides that are involved in the interaction with 40S subunits by footprinting of binary IRES–40S subunit complexes. Interaction sites were identified in domain $IIId_1$, in the pseudoknot, and flanking the initiation codon. Mutational analysis of regions of the IRES that included these contact sites confirmed their importance for ribosomal binding and thus for IRES-mediated initiation. These observations are consistent with a model for IRES function in which ribosomal binding involves multiple interactions between the 40S subunit and the IRES.

RESULTS

Localization of 40S subunit binding sites on the IRES by enzymatic footprinting

A fundamental aspect of initiation on the CSFV IRES is its ability to bind 40S subunits in the absence of factors to form stable binary complexes. Sites at which 40S subunits bind the IRES were identified by footprinting, using an approximately threefold molar excess of 40S subunits, buffer conditions appropriate for CSFV translation, and either RNase V_1 (which cleaves base-paired or stacked RNA) or RNase T_1 (which cleaves RNA after unpaired G residues) (Ehresmann et al., 1987). Enzymatic cleavage of RNA is detected by arrest of primer extension at the nucleotide on the 3′ side of the cleaved bond, and numbering refers to this nucleotide. Results of this analysis are summarized in Figure 1.

40S subunits protected the IRES from RNase V_1 cleavage at G_{263} and $UC_{285–6}$ in domain III and at C_{372}, U_{380}, A_{386}, and $UUG_{389–391}$ downstream of the pseudoknot (Fig. 2A). Residues $UUG_{389–391}$ are downstream of the initiation codon $AUG_{373–375}$ and overlap the toeprints at $UUU_{387–389}$ caused by 40S subunits bound to the IRES (Pestova et al., 1998b). RNase V_1 cleavage at C_{251}, A_{336}, and U_{387} was enhanced in binary complexes. Some residues that appear to be protected by 40S subunits from cleavage coincide with strong stops formed during primer extension on this highly structured RNA. Protection of such residues is therefore equivocal and is not discussed. Footprint analysis of domain II and the 5′ half of domain III using different primers did not reveal any additional sites protected from RNase V_1 cleavage (data not shown).

40S subunits protected the IRES from RNase T_1 cleavage at U_{192} in IIIb, at $GGU_{269–271}$ in the apical loop of $IIId_1$, weakly at U_{140} and A_{327} in the pseudoknot, strongly at U_{363} and $GC_{369–370}$, and more weakly at $GA_{376–377}$ and U_{379} downstream of the pseudoknot (Fig. 2B,C). RNase T_1 cleavage at $GGC_{63–65}$, A_{220}, and C_{338} was enhanced in binary complexes. These sites of altered RNase T_1 cleavage correlate with the sites of altered RNase V_1 cleavage. No additional sites of altered RNase T_1 cleavage were identified in domain II or in the 5′ half of domain III under the conditions of these experiments.

The accessibility of sites in the CSFV pseudoknot to cleavage by RNase T_1 at sites that are also cleaved by RNase V_1 is consistent with an earlier report regarding cleavage of the HCV pseudoknot by these two RNAses (Wang et al., 1995). Taken together, these observations suggest that the pseudoknot in these IRESs is not a static structure.

Structure of mutant CSFV IRESs

Footprinting indicated that the 40S subunit interacts with sites that include $IIId_1$, the pseudoknot, and residues flanking the initiation codon. To investigate the importance of these interactions, the IRES (Fig. 3) was mutated at or near protected residues and at residues that are structurally important or conserved in CSFV-like IRESs (Lemon & Honda, 1997; Hellen & Pestova, 1999). We assayed the effect of mutations on IRES-mediated translation in vitro and on intermediate steps in initiation, from binding of the IRES to 40S subunits up to 48S complex formation. A series of deletions was also made to identify the minimal IRES fragment that can bind 40S subunits: nt 1–127 (domains I and II)

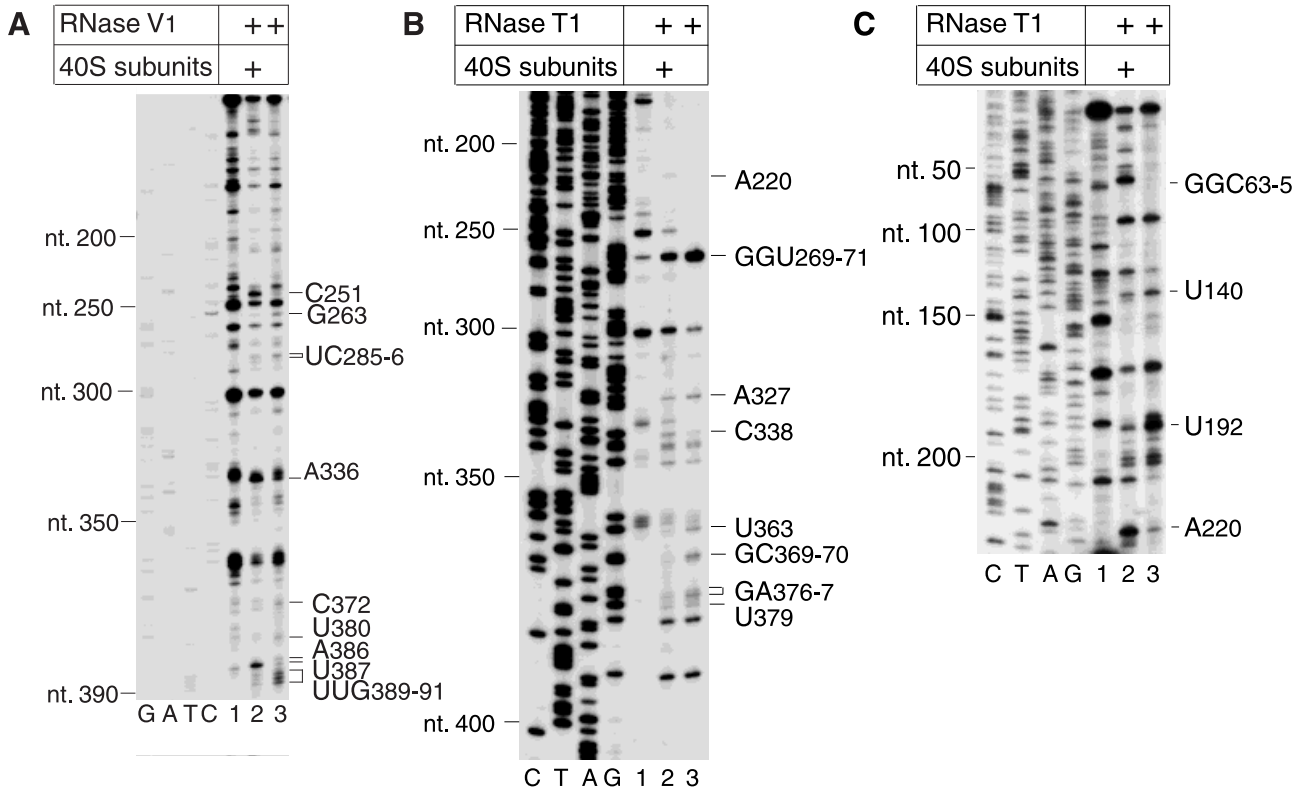

FIGURE 2. Enzymatic footprinting of the CSFV IRES–40S subunit complex. Gel fractionation of cDNA products obtained by primer extension showing the sensitivity of CSFV RNA upstream of nt 400 to RNase V_1 cleavage (**A**), the sensitivity of RNA upstream of nt 405 to RNase T_1 cleavage (**B**), and the sensitivity of RNA upstream of nt 224 to RNase T_1 cleavage (**C**), in each instance either alone (lane 3) or complexed with 40S subunits (lane 2). cDNA products obtained after primer extension of untreated RNA are shown in lane 1 of **A**–**C**. A dideoxynucleotide sequence generated with the same primer was run in parallel on each gel. The positions of protected residues are indicated to the right of each panel, and of CSFV nucleotides at 50 nt intervals to the left of each panel.

were deleted alone or with internal deletions of nt 182–234 (IIIb), nt 235–244 (IIIc) and nt 164–244 (IIIa, IIIb, and IIIc).

The effect of mutations on IRES structure was determined by RNase probing. Deletion of nt 1–127 had no effect on the cleavage pattern in the remainder of the IRES (not shown) and further deletion of nt 182–234 did not alter cleavage in domain III or in the pseudoknot (Fig. 4G). A few mutations altered the pattern of cleavage in the pseudoknot and adjacent structures. The substitution $CCA_{331–3}GGU$ enhanced RNase T_1 cleavage weakly at A_{313}, $GGU_{317–319}$, C_{321}, and at the mutated residues $GU_{332–333}$, strongly at A_{308}, $GC_{341–342}$, and U_{346}, and abrogated cleavage at A_{327} (Fig. 4C). These changes are all close to the helix in the pseudoknot that was disrupted by this mutation. However, a similar set of changes was also caused by mutations in two more distal IRES subdomains. The deletion $\Delta GGG_{268–70}$ in $IIId_1$ enhanced cleavage moderately at A_{308} and strongly at A_{313} and $GGU_{317–319}$, but reduced cleavage at A_{327} (Fig. 4D; lanes 7 and 9). Similar but less pronounced changes were also caused by mutations $GGG_{268–270}CCC$ in $IIId_1$, and $\Delta GU_{171–172}$ and $AA_{162–163}CU$ in IIIa (Fig. 4F, lanes 7 and 9; Fig. 4B; Fig. 4F, lanes 4–6, respectively). Cleavage at A_{313} was enhanced by deletion of nt 145–148 (Fig. 4A, lanes 4 and 6). No significant alteration in the pattern of cleavage was detected for the $A_{305}U$ and $\Delta AU_{313–314}$ mutants (Fig. 4E). These alterations in the cleavage pattern of mutant IRESs in the absence of 40S subunits are summarized in Figure 4H.

The pattern of RNase V_1 cleavage of the IRES was not significantly altered by deletion of either nt 171–172 or nt 1–127/182–234 (e.g., Fig. 5A). Cleavage of the $AA_{162–163}CU$ mutant was enhanced at G_{307} but otherwise occurred at the same sites as on the wild-type IRES (Fig. 5B).

Most mutations caused little or no change to the sensitivity of the IRES to cleavage other than in the immediate vicinity of mutations that, therefore, did not cause major structural changes. Subdomains $IIId_1$ and to a lesser extent IIIa appear to influence the structure of the pseudoknot and of IIIe, possibly as a consequence of tertiary interactions.

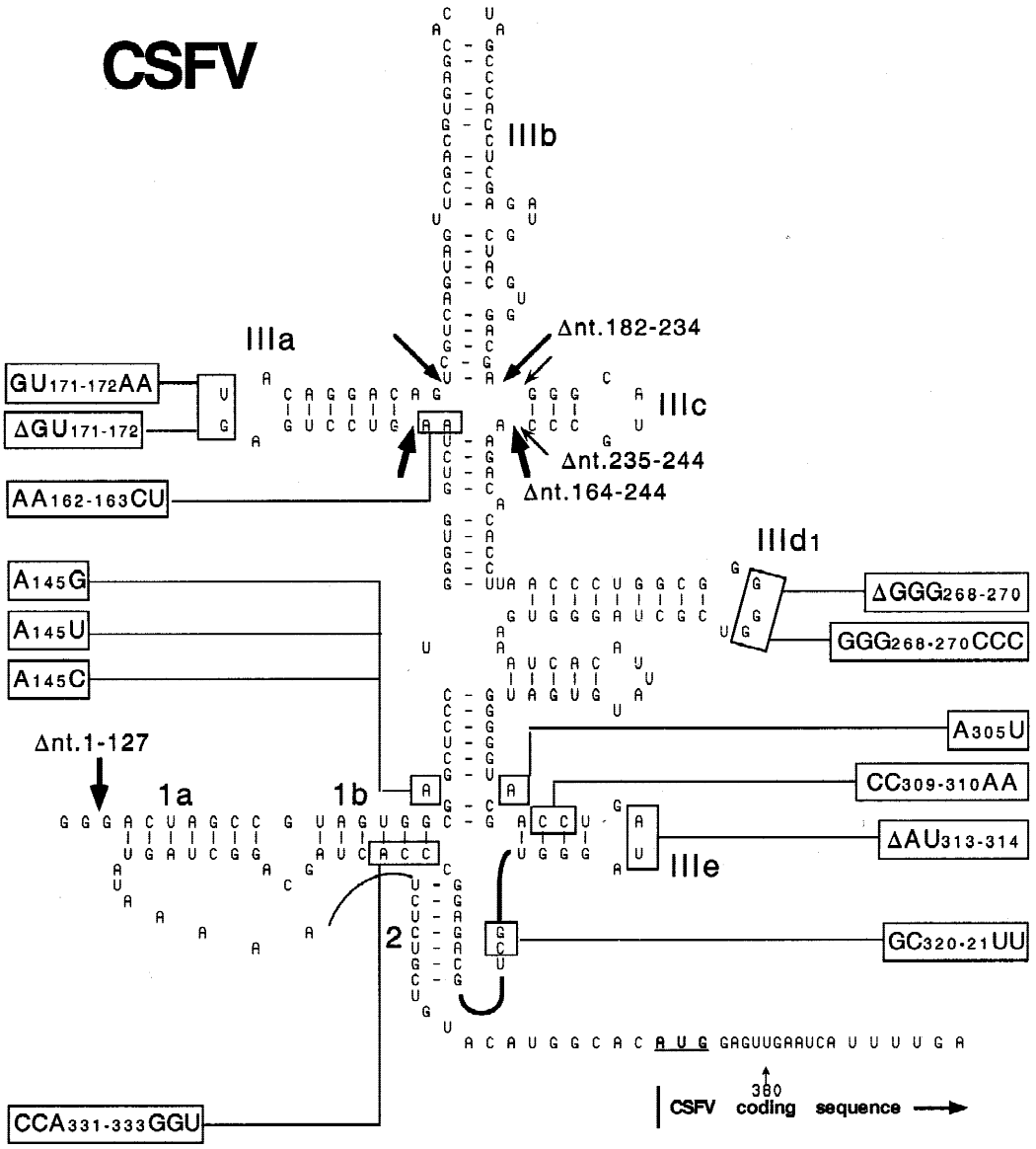

FIGURE 3. Schematic representation of the secondary structure of nt 126–392 of the CSFV IRES showing the positions of mutations. The 5′ and 3′ borders of nt 164–244, nt 182–234, and nt 235–244 deletions are indicated by matching arrows, and the 3′ border of the nt 1–127 deletion is indicated by a bold arrow. The initiation codon ($AUG_{373–375}$) is underlined.

Translation activity of mutant CSFV IRESs

IRES-mediated translation was almost abolished by substitution or deletion of the apical residues in $IIId_1$ that were protected from RNase T_1 cleavage by bound 40S subunits (Fig. 6 and Table 1). Translation was also strongly impaired by disruption of pseudoknot helix 1b in mutant $CCA_{331–333}GGU$. Base pairing in pseudoknot helix 2 is also essential for translation (Pestova et al., 1998b). An A-A mispair is adjacent to the pseudoknot in all CSFV-like IRESs and substitution of either A_{145} or A_{305} reduced translation two- to threefold. Subdomain IIIe and the residues connecting it to pseudoknot helix 2 are also conserved but surprisingly, substitution ($CC_{309–310}AA$) and deletion ($\Delta AU_{313–314}$) of residues in this region had little effect on translation. By way of comparison, deletion of IIIe had little effect on BVDV IRES function (Chon et al., 1998), whereas substitutions or a 2-nt deletion in IIIe of the HCV IRES abrogated its activity (Psaridi et al., 1999). The conformation of IIIa was important for IRES function: the substitution $AA_{162–163}CU$ (which is predicted to extend the IIIa helix by 2 bp) and the deletion of the apical residues $GU_{171–172}$ both reduced translation about 10-fold, whereas the substitution $GU_{171–172}AA$ had little effect.

Deletion of domains I and II led to a minor reduction in translation, indicating that they contribute to

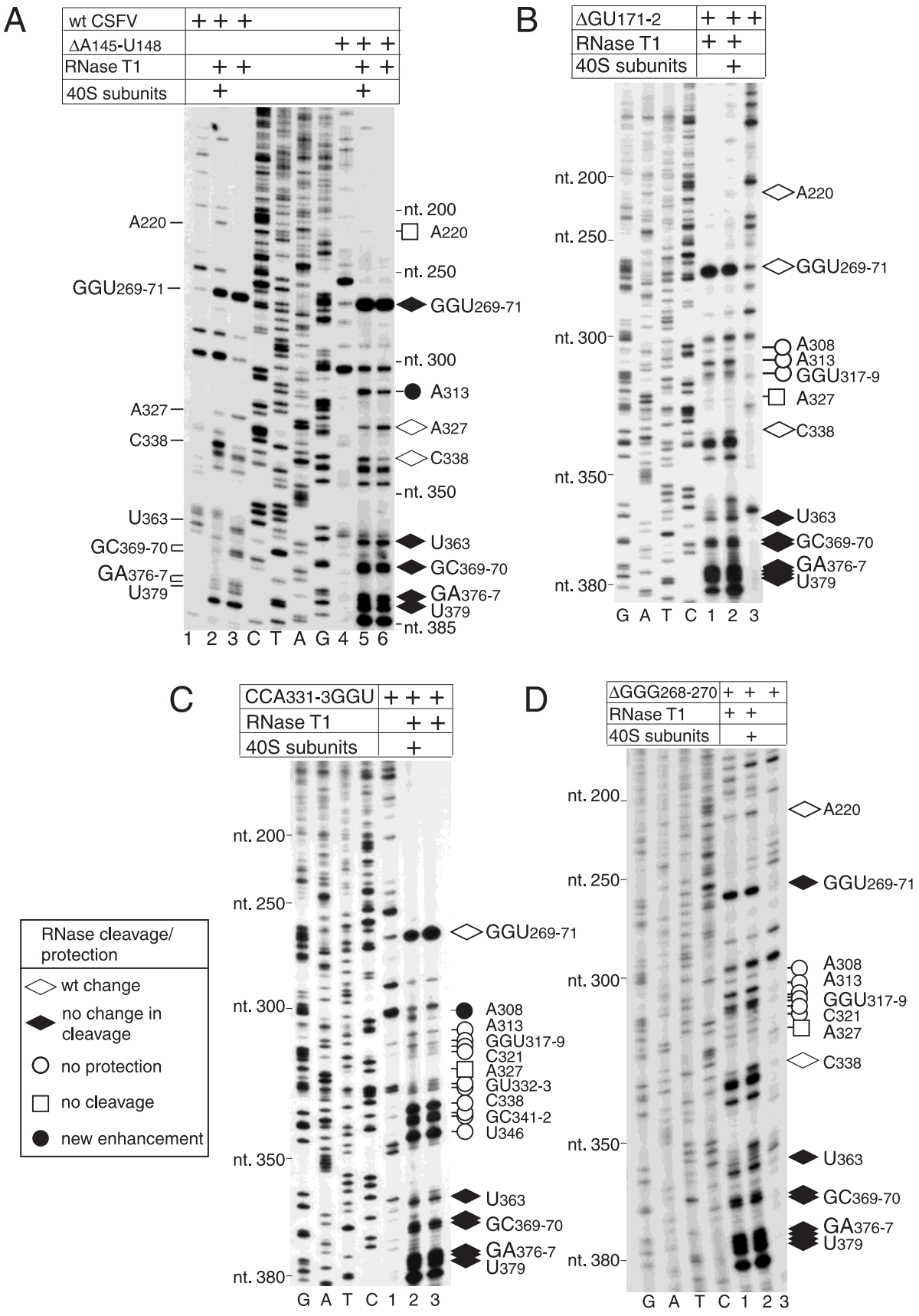

FIGURE 4. RNase T_1 footprinting of complexes formed by binding of 40S subunits to the wild-type CSFV IRES (**A**,**F**, lanes 1–3) and mutant IRESs (**A**–**G**). Mutated RNAs contain deletion Δnt 145–8 (**A**, lanes 4–6), deletion $GU_{171–172}$ (**B**), substitution $CCA_{331–333}GGU$ (**C**), deletion $\Delta GGG_{268–270}$ (**D**).

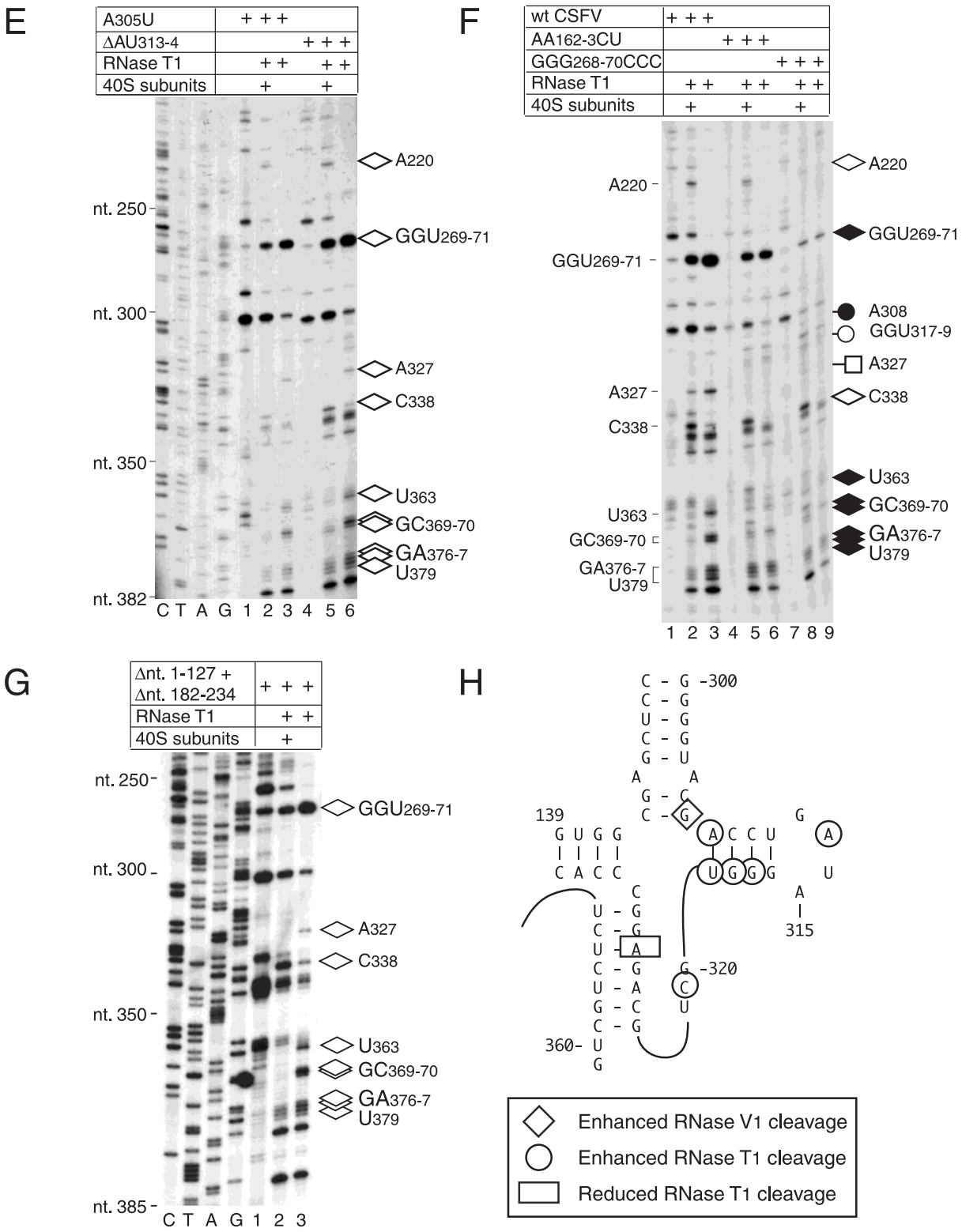

FIGURE 4. Substitution $A_{305}U$ (**E**, lanes 1–3) and deletion $\Delta AU_{313–314}$ (**E**, lanes 4–6), substitution $AA_{162–163}CU$ (**F**, lanes 4–6) and substitution $GGG_{268–270}CCC$ (**F**, lanes 7–9), and deletion Δnt 1–127/nt 182–234 (**G**). **A**–**G** show gel fractionated cDNAs obtained by primer extension of untreated CSFV RNA or of RNA either alone or complexed with 40S subunits after cleavage by RNase T_1, as indicated. A dideoxynucleotide sequence generated with the same primer was run in parallel on each gel. The positions of protected residues and of CSFV nucleotides at 50 nt intervals are indicated on each panel. Sites of cleavage and protection are compared to wild-type RNA according to the symbols tabulated at the lower left of **C**. A summary of sites of altered susceptibility to cleavage by RNases T_1 and V_1 is shown in **H**.

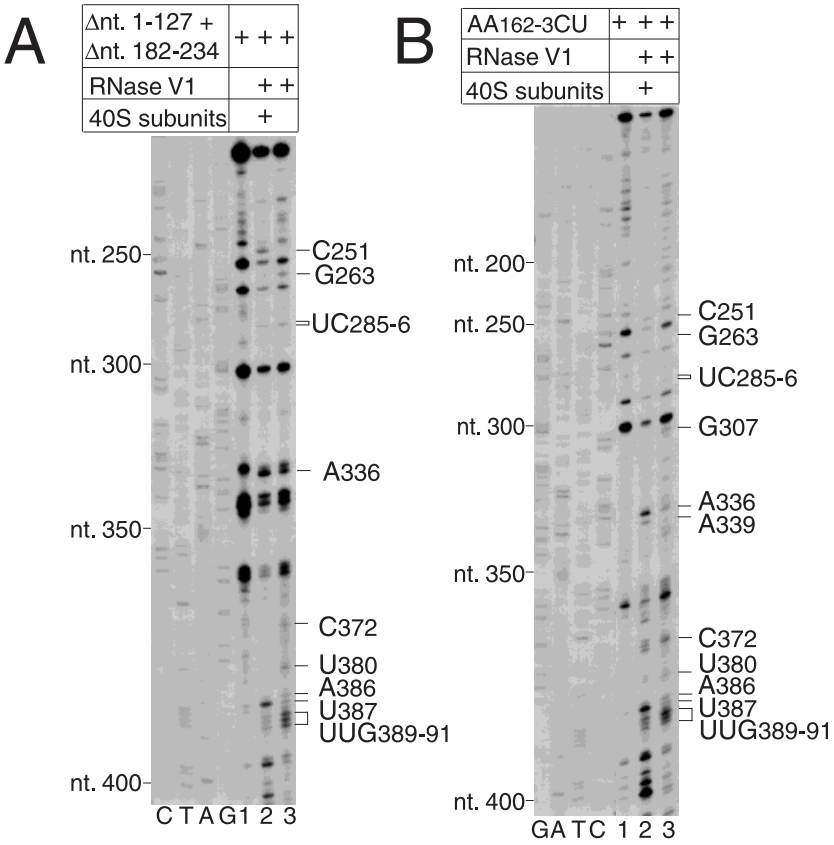

FIGURE 5. RNase V_1 footprinting of complexes formed by binding of 40S subunits to mutant IRESs containing deletion Δnt 1–127/nt 182–234 (**A**) and substitution $AA_{162–3}CU$ (**B**). These panels show gel fractionated cDNA products obtained by primer extension of untreated RNA (lane 1) or of RNA either alone (lane 3) or complexed with 40S subunits (lane 2) after RNase V_1 cleavage, as indicated. A dideoxynucleotide sequence generated with the same primer was run in parallel on each gel. The positions of protected residues are indicated to the right of each panel, and of CSFV nucleotides at 50 nt intervals to the left of each panel.

but are not essential for IRES function. These domains are also not essential for initiation on the HCV IRES (Tsukiyama-Kohara et al., 1992; Kamoshita et al., 1997; Psaridi et al., 1999). Surprisingly, a CSFV IRES mutant lacking domains I and II but with an additional ($A_{145}U$) lesion was almost wholly inactive in mediating translation, even though individually these mutations had only minor effects on translation efficiency. Translation mediated by IRES mutants with deletions of nt 182–234 (IIIb), nt 235–244 (IIIc), or nt 164–244 (IIIa, IIIb, and IIIc) in addition to the nt 1–127 deletion was significantly lower than translation mediated by the wild-type IRES (Fig. 6C). Initiation mediated by the IRES is resistant to inhibition by R362Q mutant eIF4A, which is a *trans*-dominant inhibitor of cap-mediated translation (Pause et al., 1994). To verify that the residual activity detected on translation of mutant RNAs was not due to end-dependent translation of fragmented RNA, eIF4A (R362Q) was included in parallel translation reactions. It had no effect on residual translation activity (e.g., Fig. 6E). These observations indicate that IIIa, IIIb, and IIIc all contain important determinants of IRES function; they are consistent with the effects on IRES function of individual destabilizing mutations in these subdomains.

Footprinting analysis of the interaction of 40S subunits with mutant IRESs

Footprinting indicated that 40S subunits binds directly to $IIId_1$, to the pseudoknot, and extensively to residues flanking the initiation codon. Footprinting was next used to map the interaction of 40S subunits with IRES variants that had been mutated at these and other regions. Protection by 40S subunits from RNase T_1 and V_1 cleavage of a mutant lacking nt 1–127/182–234 was similar at all positions to the pattern of protection on the wild-type IRES (Figs. 4G, 5A). A Δnt 145–8 mutant IRES was protected by 40S subunits from RNase T_1 cleavage only at A_{327} (Fig. 4A, lanes 4–6). No part of those mutant IRESs that had either a deletion ($\Delta GGG_{268–270}$) or substitution ($GGG_{268–270}CCC$) in $IIId_1$ was protected by 40S subunits from RNase T_1 cleavage (Fig. 4D; Fig. 4F, lanes 7–9). The apical loop of $IIId_1$ is thus a primary determinant of stable binding of 40S subunits to the IRES.

The apical residues $GGU_{269–271}$ in $IIId_1$ were strongly protected from RNase T_1 cleavage when 40S subunits bound to the $CCA_{331–333}GGU$ mutant (in which helix 1b of the pseudoknot is disrupted) but no protection was observed in or downstream of the pseudoknot (Fig. 4C). This apical loop was partially protected

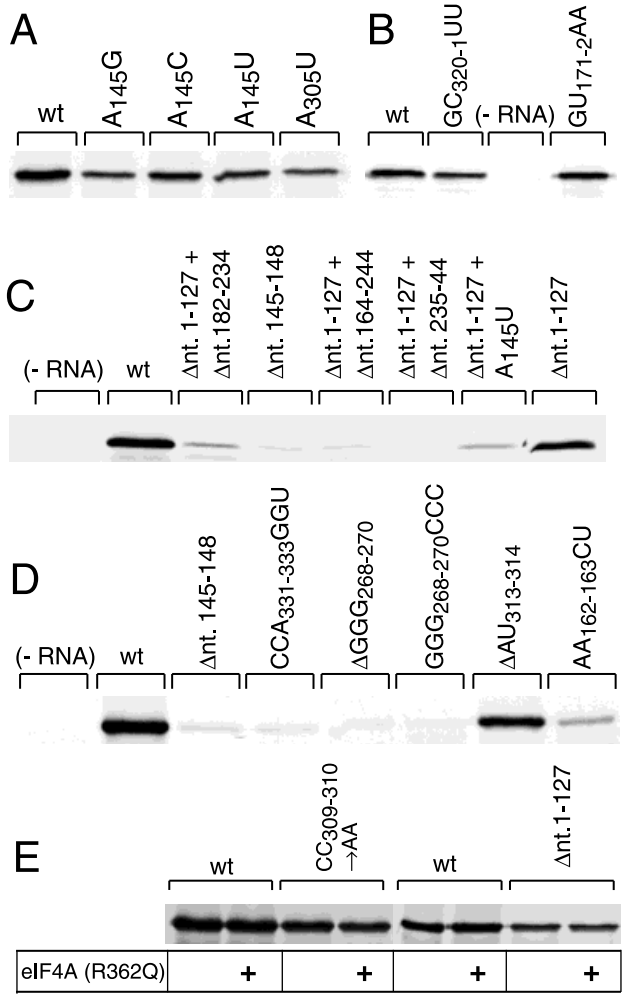

FIGURE 6. Translation of CSFV(1–442)-NS′ mutant RNAs. RNAs were translated in rabbit reticulocyte lysate, and aliquots of the translation reaction mixture were separated by electrophoresis on 12% polyacrylamide gel. Lanes are labeled to indicate either the wild-type (wt) or the mutant RNA (as defined in Table 1) used to program translation of NS′ polypeptide. Lanes labeled (−RNA) correspond to lysate programmed without exogenous mRNA. eIF4A (R362Q) was added to translation reactions in **E** as indicated.

TABLE 1. Effects of mutations in different structural elements of the CSFV IRES on its activity in mediating translation in vitro.

Structural element	Mutation	Translation activity[a]
	Δnt 1–127	62%
	Δnt 1–127 + A145U	6%
	Δnt 1–127 + Δnt 182–234	9%
	Δnt 1–127 + Δnt 235–244	<1%
	Δnt 1–127 + Δnt 164–244	<1%
A-A mispair	$A_{145}G$	41%
	$A_{145}U$	66%
	$A_{145}C$	51%
	$A_{305}U$	33%
Pseudoknot	$CCA_{331–333}GGU$	2%
	Δnt 145–148	<1%
IIIa	$AA_{162–163}CU$	9%
	$GU_{171–172}AA$	85%
	$\Delta GU_{171–172}$	6%
$IIId_1$	$GGG_{268–270}CCC$	<1%
	$\Delta GGG_{268–270}$	<1%
IIIe	$CC_{309–310}AA$	57%
	$\Delta AU_{313–314}$	47%
	$GC_{320–321}UU$	71%

[a]Values represent synthesis of the NS′ reporter by IRES mutants as a percentage of the value for the wild-type IRES, and are the mean of three assays.

from RNase T_1 cleavage when 40S subunits bound to $AA_{162–163}CU$ and $\Delta GU_{171–172}$ mutants and cleavage at A_{220} was enhanced (Fig. 4B, lanes 1 and 2; Fig. 4F, lanes 5 and 6). There was no RNase T_1 cleavage and thus no possibility of detecting protection in the pseudoknot, but there was no protection from RNase T_1 cleavage elsewhere, and cleavage by RNase V_1 in and downstream of the pseudoknot was much weaker than on the wild-type IRES (Fig. 4B; Fig. 4F, lanes 4–6; Fig. 5B). No significant differences in the pattern of protection by 40S subunits were detected between the wild-type IRES and the $A_{305}U$ and $\Delta AU_{313–314}$ mutants (Fig. 4E). These results suggest that $IIId_1$ can interact with 40S subunits independently of other interactions that are required for stable binding of 40S subunits at the initiation codon. They also suggest that subdomain IIIa influences ribosomal association with residues downstream of the pseudoknot.

Assembly of binary ribosomal complexes on the IRES

Formation of stable binary complexes by binding of 40S subunits to the IRES can be assayed by primer extension inhibition (“toeprinting”) and by sucrose density gradient centrifugation (Pestova et al., 1998b). Both methods were used to assay the interaction of the IRES mutants described above with 40S subunits.

Primer extension is arrested at C_{334} and at $UUU_{387–389}$ in binary complexes formed on the wild-type IRES (e.g., Fig. 7A, lanes 1 and 2) (Pestova et al., 1998b). The C_{334} toeprint was abolished and the $UUU_{387–389}$ toeprints were strongly reduced when binary complexes were assembled on mutant IRESs in which $GGG_{268–270}$ had been deleted or substituted (Fig. 7F, lanes 4, 5, 7, and 8). Sucrose density gradient centrifugation analysis confirmed that the stability of binary complexes formed on the $GGG_{268–270}CCC$ mutant and to a greater extent on the $\Delta GGG_{268–270}$ mutant was strongly reduced (Fig. 8B).

Two mutations in IIIa also strongly reduced ribosomal binding to the IRES: deletion of $GU_{171–172}$ in the apical loop of IIIa and a $AA_{162–163}CU$ substitution at its base both abrogated the C_{334} toeprint and strongly re-

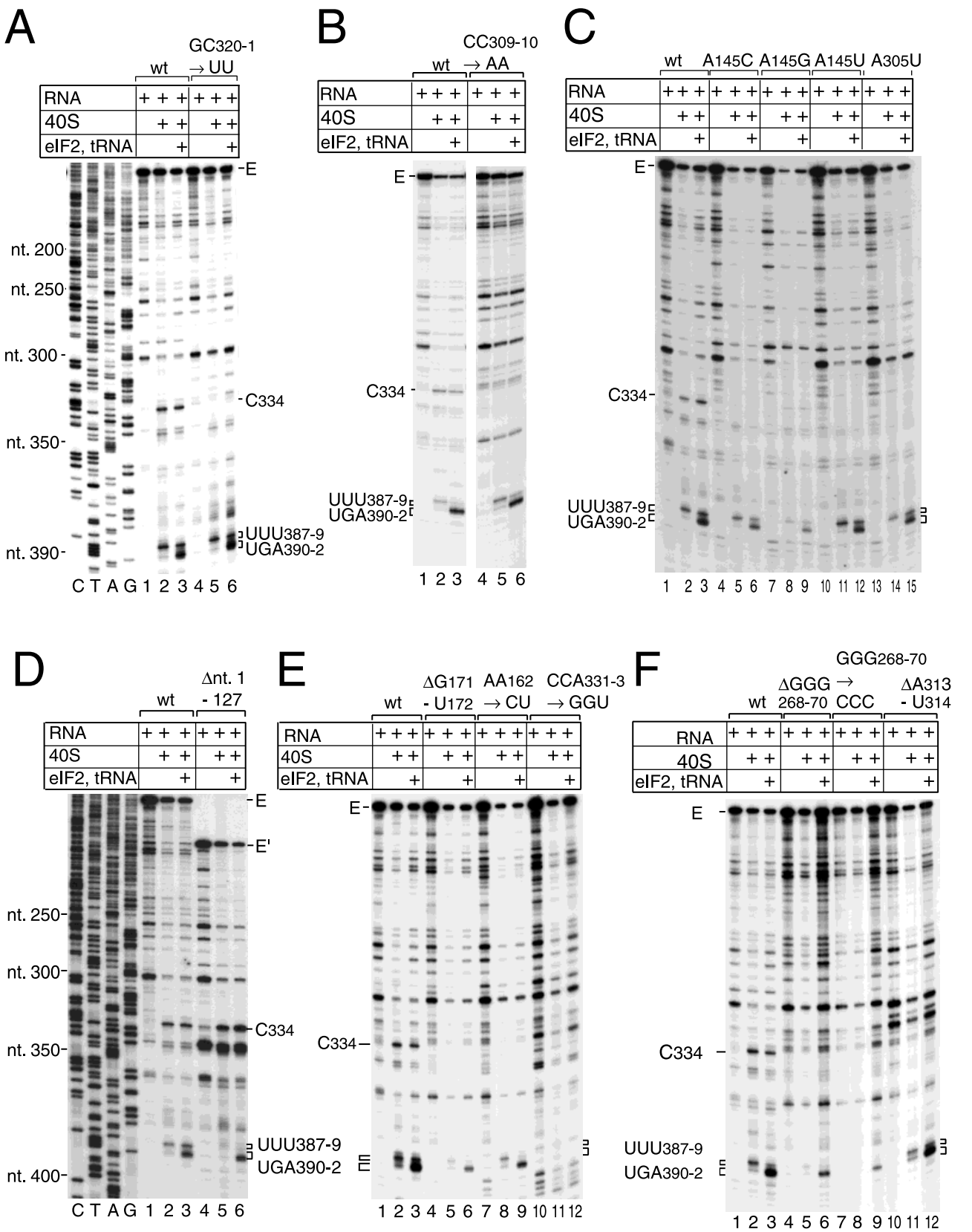

FIGURE 7. Toeprint analysis of 48S complexes assembled on mutant CSFV IRESs. Ribosomal preinitiation complexes were assembled on mutant CSFV (nt 1–442)-NS′ RNA (**A**–**C**, **E**, **F**), CSFV (nt 128–442)-NS′ RNA (**D**), and on wild-type CSFV (nt 1–442)-NS′ RNA under standard reaction conditions in the presence of translation components as indicated and were then analyzed by primer extension. Full-length cDNA is marked E and other cDNAs terminated at the sites indicated on the right. Reference lanes C, T, A, and G depict CSFV sequences; CSFV nucleotides are indicated to the left of **A** and **D**.

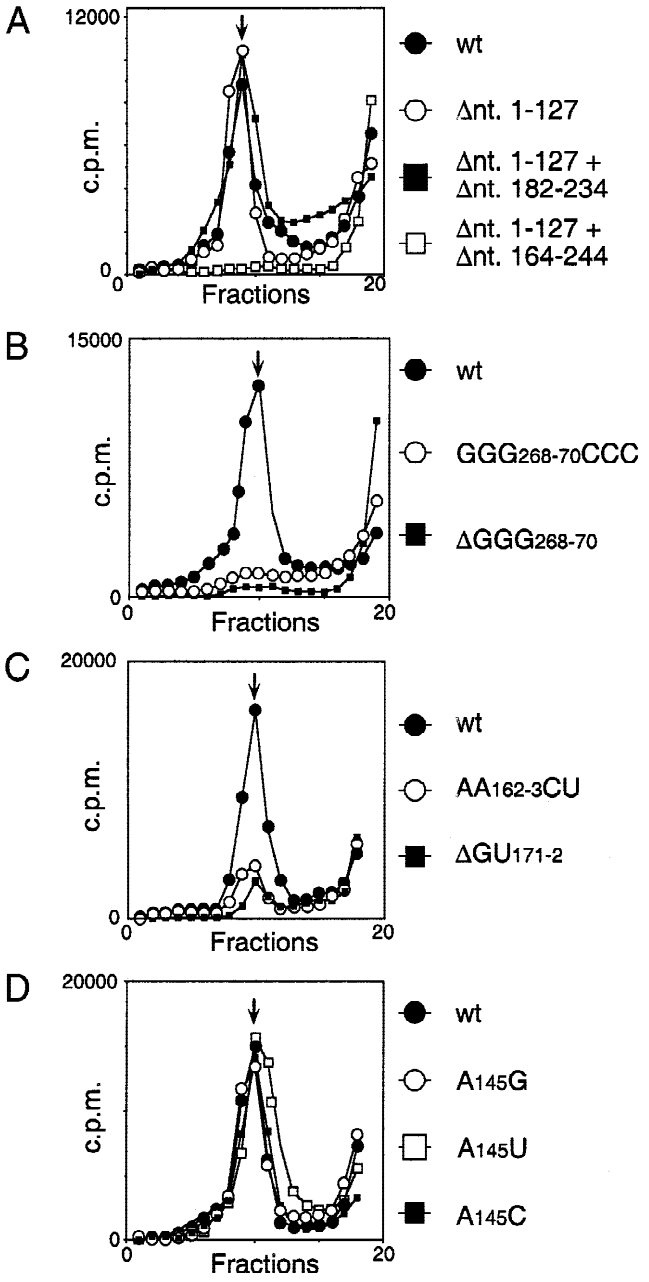

FIGURE 8. Binary ribosomal complex formation on the CSFV IRES. Ribosomal complexes were assembled by incubating 40S subunits with either wild-type or mutant [^{32}P]-UTP-labeled CSFV mRNAs as indicated and were analyzed by sucrose density gradient centrifugation. Sedimentation was from right to left. The positions of binary IRES-40S subunit complexes are indicated by arrows. Fractions from the upper part of sucrose gradients have been omitted for clarity.

duced the $UUU_{387–389}$ toeprints (Fig. 7E, lanes 4, 5, 7, and 8). Binary complexes that assembled on these mutant IRESs were less stable than complexes formed on the wild-type IRES (Fig. 8C). However, substitution ($GU_{171–172}AA$) rather than deletion of these apical residues had little effect on binary complex formation (Fig. 9B, lanes 5 and 6).

Disruption of pseudoknot helix 1b in mutant $CCA_{331–333}GGU$ abrogated stable binding of ribosomes to the IRES as judged by sucrose density gradient centrifugation (not shown). Toeprints were not detected in the pseudoknot or at $UUU_{387–389}$ on this mutant (Fig. 7E, lanes 10 and 11). Helix 1b of the pseudoknot is thus essential for binary complex formation, in contrast to helix 2, the integrity of which is required for 48S complex formation but not for 40S subunit binding (Pestova et al., 1998b).

Mutations $CC_{309–310}AA$ and $\Delta AU_{313–314}$ in IIIe and $GC_{320–321}UU$ in an adjacent loop did not alter the toeprints at $UUU_{387–389}$, but strongly reduced or even abrogated the C_{334} toeprint (Fig. 7A,B, lanes 4 and 5; Fig. 7F, lanes 10 and 11; Fig. 9A, lanes 5 and 7). Substitution of either of the mispaired residues A_{145} and A_{305} near the pseudoknot had effects on ribosomal binding similar to those of the mutations in IIIe. The intensity of the toeprint in the pseudoknot was strongly reduced, but the intensity of toeprints downstream of the initiation codon was not significantly affected (Fig. 7C, lanes 4, 5, 7, 8, 10, 11, 13, and 14). Nevertheless, the binary 40S subunit–IRES complexes that formed on $A_{145}G$, $A_{145}U$, and $A_{145}C$ mutant IRESs were stable as judged by sucrose density gradient centrifugation (Fig. 8D).

Finally, we made a series of deletions to identify the minimal IRES fragment that is able to bind stably to 40S subunits. The interaction with 40S subunits of RNAs lacking nt 1–127 either alone or in addition to deletions of nt 182–234, nt 235–244, or nt 164–244 was defective, because bound 40S subunits either yielded anomalous toeprint patterns or formed weaker binary complexes than on the wild-type IRES. 40S subunits bound to the Δnt 1–127 mutant yielded a toeprint at C_{334} in the pseudoknot that was comparable to that on the wild-type IRES, stronger toeprints at $GUUG_{378–381}$, but much weaker toeprints at $UUU_{387–389}$ (Fig. 7D, lanes 4 and 5; Fig. 9C, lanes 3 and 4). A prominent toeprint was also detected at C_{334} when 40S subunits were incubated with Δnt 1–127/235–244 and Δnt 1–127/182–234, but not Δnt 1–127/164–244 mutant RNAs; the $UUU_{387–389}$ toeprints were almost completely absent on all three of these RNAs (Fig. 9C, lanes 5–10). Stable binary complexes were formed on all mutant RNAs except for Δnt 1–127/164–244 (Fig. 8A). These results suggest that subdomain IIIa (nt 164–181) contains an essential determinant of ribosomal binding (consistent with the analysis of $\Delta GU_{171–172}$ and $AA_{162–163}CU$ mutants). The observation that the toeprints at $UUU_{387–389}$ were weakened as a result of deletion of nt 1–127 suggests that this region of the IRES may influence the correct positioning of the initiation codon in the ribosomal P site. A similar role for the corresponding region of the HCV IRES has also been suggested (Kolupaeva et al., 2000).

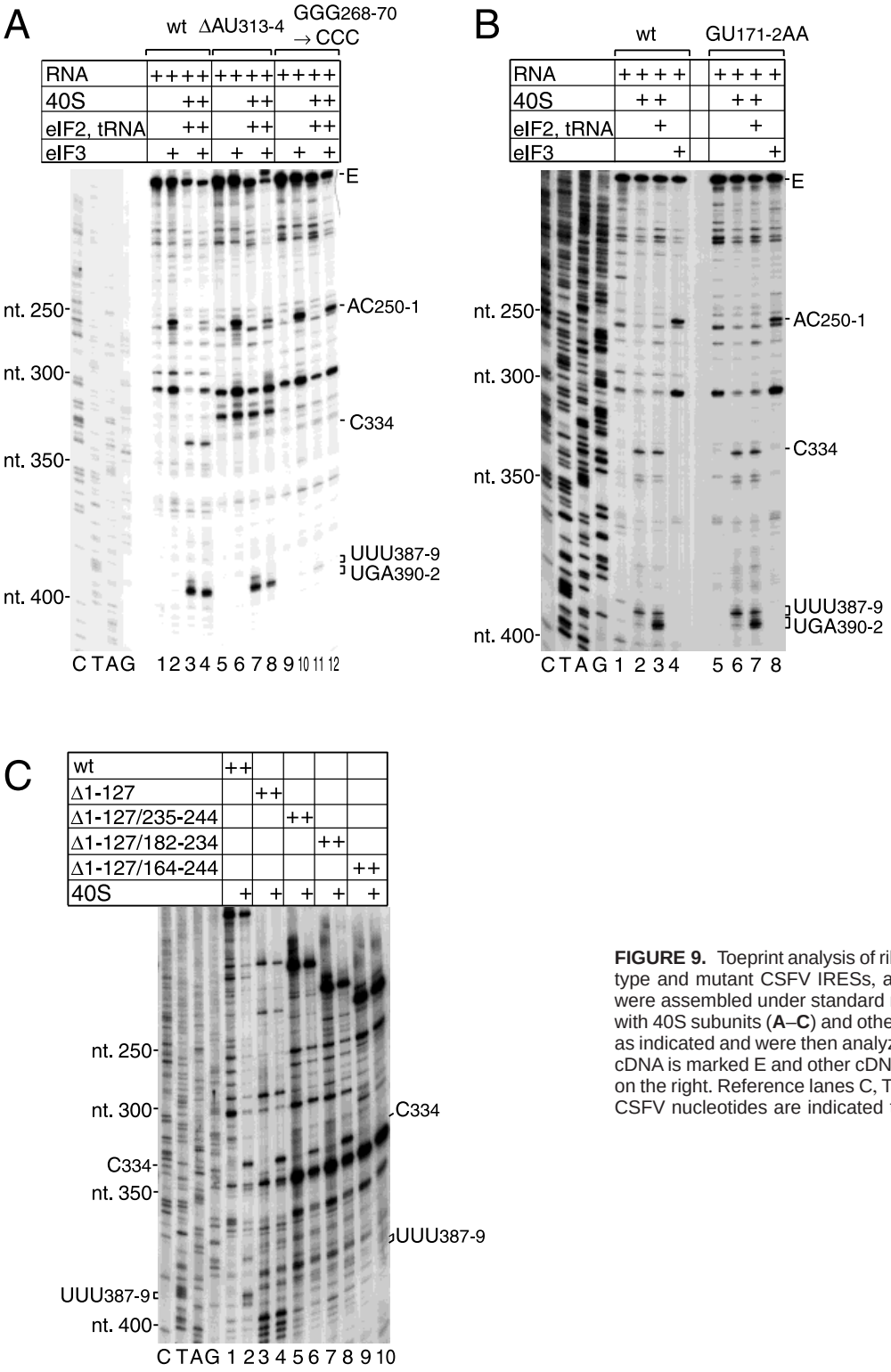

FIGURE 9. Toeprint analysis of ribosomal complex formation on wild-type and mutant CSFV IRESs, as indicated. Ribosomal complexes were assembled under standard reaction conditions on CSFV RNAs with 40S subunits (**A**–**C**) and other translation components (**A** and **B**) as indicated and were then analyzed by primer extension. Full-length cDNA is marked E and other cDNAs terminated at the sites indicated on the right. Reference lanes C, T, A, and G depict CSFV sequences; CSFV nucleotides are indicated to the left.

Interaction of eIF3 with mutant CSFV IRESs

Initiation factor eIF3 binds stably to the apical half of domain III of CSFV-like IRESs (Pestova et al., 1998b; Sizova et al., 1998). Binding of eIF3 to the wild-type IRES is sufficiently stable to be detectable by primer extension inhibition, yielding a characteristic toeprint at $AC_{250–251}$ (Fig. 9B, lanes 1 and 4; Fig. 10A–F, lanes 1 and 2). Formation of this toeprint was not affected by deletion of nt 1–127 (Fig. 10A, lanes 3 and 4) but was

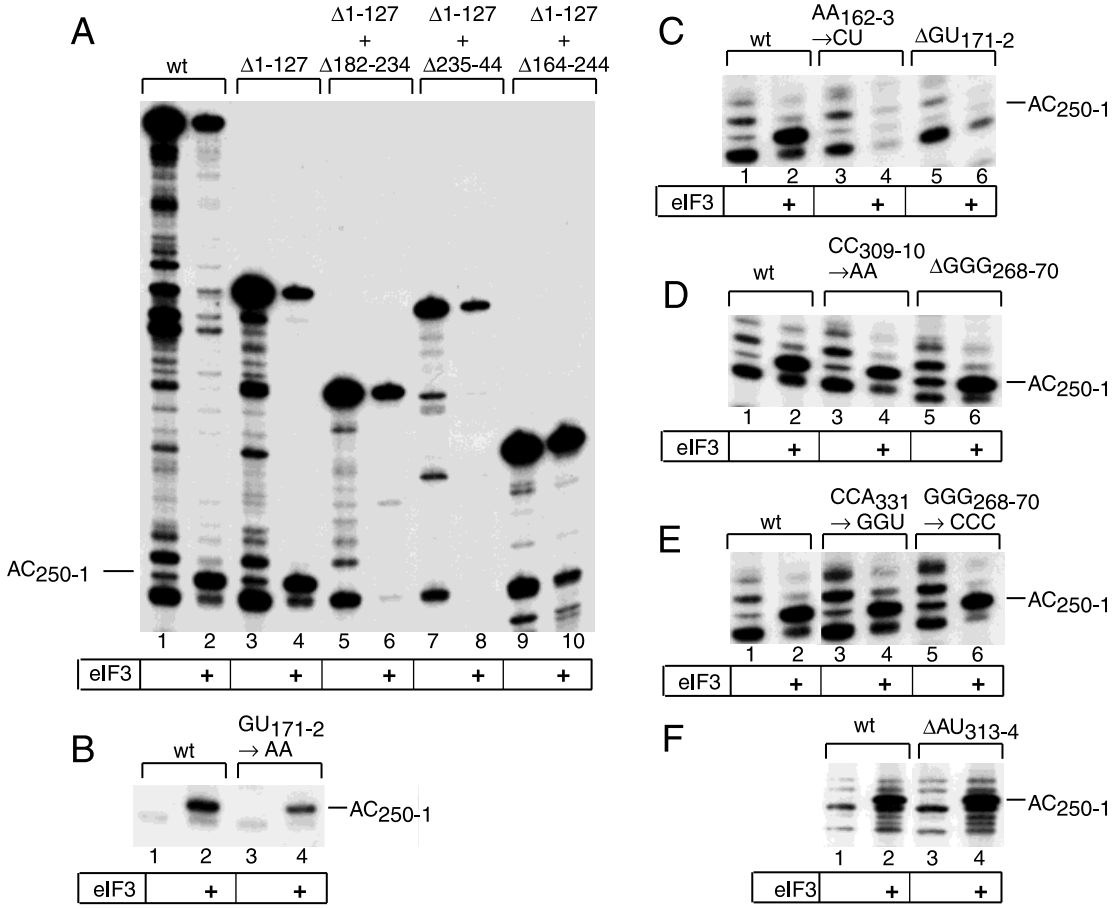

FIGURE 10. Primer extension analysis of ribonucleoprotein complexes formed on wild-type and mutant CSFV IRESs, as indicated. CSFV (nt 1–442)-NS′ RNAs were incubated with or without eIF3 (as indicated) under standard conditions. Primers were annealed to the NS′ coding sequence of these RNAs and extended with reverse transcriptase. The cDNAs labeled $AC_{250–251}$ terminated at these nucleotides. The gels shown in **B**–**F** have been truncated for clarity.

not apparent on mutant IRESs additionally lacking nt 235–244, nt 182–234, or nt 164–244 (Fig. 10A, lanes 5–10). These results are wholly consistent with the effects of analogous deletions in the HCV IRES (Pestova et al., 1998b; Sizova et al., 1998) and taken together indicate that the integrity of the apical half of domain III is required for stable binding of eIF3. Analysis of the interaction of eIF3 with other mutant IRESs (Fig. 3) supported this conclusion: binding of eIF3 was abrogated only by the $\Delta GU_{171–172}$ and $AA_{162–163}CU$ mutations (Fig. 10C, lanes 3–6) but not by the $GU_{171–172}AA$ mutation in the apical loop of IIIa (Fig. 9B, lanes 5 and 8) or by any other mutation elsewhere in the IRES (Fig. 9A, lanes 5, 6, 9, and 10; Fig. 10D–F). These results indicate that domain IIIa is important both for the binding of eIF3 and of 40S subunits to the IRES.

48S complex formation on mutant IRESs

The results reported here and elsewhere (Pestova et al., 1998b) suggest that the IRES contains one group of determinants (including IIIa and $IIId_1$ and pseudoknot helix 1b) that are needed to bind 40S subunits and a second group (including domain II, pseudoknot helix 2, and nucleotides 3′ of the pseudoknot) that are directly or indirectly required to position the initiation codon in the ribosomal P site. We used toeprinting to investigate the influence of mutations in these various parts of the IRES on 48S complex formation using only 40S subunits and the eIF2/GTP/initiator tRNA ternary complex. 48S complexes assembled on the wild-type IRES in this way yield prominent $UGA_{390–392}$ toeprints; the toeprints at $UUU_{387–389}$ are weaker than for binary ribosomal complexes (e.g., Fig. 7A, lanes 1 and 3).

Assembly of minimal 48S complexes from 40S subunits and the ternary eIF2/GTP/initiator tRNA complex (but lacking eIF3) was completely abrogated by the $CCA_{331–333}GGU$ pseudoknot mutation (Fig. 7E, lane 12). Disruption of IIIa and $IIId_1$ also strongly reduced but did not abolish 48S complex formation (Fig. 7E,F, lanes 6 and 9) whereas substitution ($GU_{171–172}AA$) of apical residues in IIIa had no significant effect (Fig. 9B,

lanes 5–7). 48S complex formation was also not significantly affected by mutations in IIIe and adjacent residues (Fig. 7A,B lanes 6; Fig. 7C, lanes 6, 9, 12, and 15; Fig. 7F, lane 12; Fig. 9A, lane 7). The toeprints at $UGA_{390–392}$ that are due to bound minimal 48S complexes were stronger on several of the mutant IRESs than the toeprints at $UUU_{387–389}$ due to bound 40S subunits alone (e.g., Fig. 7F, lanes 5, 6, 8, and 9). This difference is also seen on wild-type RNA (e.g., Fig. 7F, lanes 2 and 3) and is indicative of the additional stabilizing effect that codon–anticodon base pairing has on the interactions of CSFV RNA in the mRNA-binding cleft of the 40S subunit. The effects of these mutations on 48S complex formation are generally consistent with their effects on in vitro translation (Fig. 6 and Table 1) and are in good agreement with the importance of IRES substructures identified by footprinting and toeprinting that are required to promote accurate binding of 40S subunits to the IRES. However, formation of minimal 48S complexes on some mutant IRESs was less impaired than translation in vitro.

The influence of eIF3 on 48S complex formation on these mutant IRESs was assayed because eIF3 binds specifically to them (Fig. 10) and is associated with native 40S subunits in vivo (Sundkvist & Staehelin, 1975). In 48S complexes assembled on the wild-type IRES without eIF3, prominent toeprints appear at $UGA_{390–392}$ and the $UUU_{387–389}$ toeprints are weaker than for binary complexes (e.g., Fig. 7C, lanes 2 and 3). Inclusion of eIF3 in assembly reactions did not alter the $UGA_{390–392}$ toeprints, but caused the $UUU_{387–389}$ toeprints to disappear (Fig. 9A, lanes 3 and 4). Inclusion of eIF3 in assembly reactions on the $\Delta AU_{313–314}$ mutant IRES had a similar effect on the $UUU_{387–389}$ toeprints and reduced the intensity of the $UGA_{390–392}$ toeprints (Fig. 9A, lanes 7 and 8), whereas on the $GGG_{268–270}$CCC mutant IRES, inclusion of eIF3 abrogated both sets of the already very weak toeprints. Assembly of 48S complexes in the presence of eIF3 therefore accurately reflects in vitro translation activities (Fig. 6 and Table 1).

DISCUSSION

IRESs are large, complex RNAs that bear recognition sites for components of the translational apparatus in a configuration that promotes ribosomal attachment at an internal position on an mRNA. Using the CSFV IRES as a model, we report here the identification of IRES determinants that interact directly with 40S subunits and promote their binding at the initiation codon.

Binding of the 40S ribosomal subunits to the CSFV IRES

We used enzymatic footprinting to identify ribosomal binding sites on the IRES. Sites in $IIId_1$ and $IIId_2$ as well as residues $UUG_{389–391}$ 3′ of the initiation codon were protected by 40S subunits from RNase V_1 cleavage; residues in the apical $IIId_1$ loop, in the pseudoknot, and flanking the initiation codon were protected from RNase T_1 cleavage (Fig. 1).

Conserved unpaired IRES residues have been assumed to play important roles in IRES function because of their potential for involvement in higher-order interactions (Jackson & Kaminski, 1995). We previously determined that eIF3 binds to the internal bulge in IIIb (Sizova et al., 1998) and have now identified the apical loop residues $GGG_{268–270}$ in $IIId_1$ as one of the multiple contacts between the IRES and 40S subunits. The importance of this interaction for IRES function was confirmed experimentally. Significantly, three G residues occur at an equivalent location in all CSFV-like viruses (Hellen & Pestova, 1999). The equivalent HCV residues are also protected from RNase T_1 cleavage by 40S subunits (Kolupaeva et al., 2000) and substitution of them results in near-total abrogation of IRES function (Kieft et al., 1999). The hypothesis that unpaired IRES residues interact with components of the translation apparatus is also supported by analyses of unrelated IRESs that identified loops as binding sites for eIF4G (Pestova et al., 1996b; Kolupaeva et al., 1998) and for the pyrimidine tract-binding protein (Kolupaeva et al., 1996; Pilipenko et al., 2000).

The second contact between the CSFV IRES and 40S subunits is in the pseudoknot, which has previously been identified as an important structural component of CSFV-like IRESs (Wang et al., 1994, 1995; Rijnbrand et al., 1997; Pestova et al., 1998b). Disruption of helix 1b led to additional local disruption of structure and strongly reduced binding of 40S subunits at the initiation codon, resulting in almost total loss of translation activity even though the interactions of the 40S subunit with $IIId_1$ and of eIF3 with distal regions of domain III were unaffected. The pseudoknot in CSFV-like IRESs is not static, as is evident from the cleavage by RNase T_1 of sites that are also cleaved by RNase V_1 (Wang et al., 1995; Figs. 2 and 4), and from the enhanced RNase T_1 and RNase V_1 cleavage at the internal bulge between helices 1a and 1b of the CSFV pseudoknot caused by ribosomal binding (Figs. 4 and 5). NMR spectroscopic studies of the 3′-terminal pseudoknot of turnip yellow mosaic virus suggested that it has a predisposition for partial unfolding and structural flexibility at helical junctions that may regulate protein binding (Kolk et al., 1998). Structural flexibility in CSFV-like pseudoknots may also be important for IRES function in promoting ribosomal attachment at the initiation codon, and in subsequent events in translation, for example when the ribosome detaches from the IRES during the early stages of elongation.

The third site at which 40S subunits interact with the IRES comprises residues flanking the initiation codon. Protection of these residues from RNase cleav-

age is consistent with their having been inserted into the mRNA-binding cleft of the 40S subunit, as suggested previously by toeprinting (Pestova et al., 1998b). The sequence protected from cleavage by a bound 40S subunit (nt 363–391) corresponds closely to the estimated length of the mRNA-binding cleft in eukaryotic ribosomes (Legon, 1976; Kozak, 1977; Kozak & Shatkin, 1977; Browning et al., 1980). The group of protected residues downstream of the initiation codon overlaps toeprints caused by bound 40S subunits (Pestova et al., 1998b) and therefore likely corresponds to a site that is bound near the leading edge of the ribosome. These observations suggest that residues flanking the initiation codon are likely to be in a nearly fully extended conformation. We suggest that binding of residues flanking the initiation codon of CSFV-like IRESs to a 40S subunit is a secondary consequence of primary interactions between other binding determinants in the IRES and a 40S subunit, because equivalent flanking residues in the HCV IRES are not required for it to bind stably to 40S subunits (Pestova et al., 1998b). The integrity of subdomain IIIa was necessary to stabilize this secondary interaction. A similar function can be assigned to domain II, because its deletion weakened the toeprints at $UUU_{387–389}$ at the leading edge of the bound 40S subunit in binary CSFV IRES/40S subunit complexes (Fig. 7D).

Functional importance of CSFV IRES structure

The IRES can bind eIF3 and a 40S subunit independently and all three can form a ternary complex (Pestova et al., 1998b; Sizova et al., 1998). We have now defined the interactions of both translation components with this IRES by toeprinting and footprinting: the eIF3-binding site includes IIIb and junction IIIabc (Sizova et al., 1998), whereas the 40S subunit makes more extensive contacts as described above. The results of probing HCV IRES mutants led to the proposal that this IRES contains two independent folding domains (Kieft et al., 1999) that correspond to eIF3 and 40S subunit-binding sites. Our analysis suggests that equivalent domains in the CSFV IRES are not wholly independent, and that accurate binding of a 40S subunit to this IRES also requires apical regions of domain III. Destabilizing mutations in IIIa impaired binding of 40S subunits to the pseudoknot and to residues flanking the initiation codon, and strongly reduced the stability of IRES-40S subunit complexes. IIIa therefore plays dual roles in promoting accurate binding of a 40S subunit as well as in determining stable binding of eIF3 (see below). Moreover, binding of 40S subunits to the wild-type CSFV IRES consistently resulted in protection and enhancement at single RNAse T_1 cleavage sites on opposite sides of IIIb (Figs. 1 and 2C). Analogous results have been obtained using the HCV IRES (Kolupaeva et al., 2000). The sites of enhanced cleavage coincide with sites that are protected from cleavage by eIF3 (Sizova et al., 1998).

Binding of eIF3 to the CSFV IRES is abrogated by partial or complete deletion of IIIa, IIIb, and IIIc, as well as by mutations that likely disrupt the structure of IIIa or of the IIIabc junction (Fig. 10A,C). The importance of this interaction is evident from the severe impairment of IRES function caused by these mutations, even in instances when binding of 40S subunits was not abrogated (Figs. 8A and 9C). Inclusion of eIF3 in 48S complex assembly reactions alters the toeprint pattern at the initiation codon due to bound complexes. We suggest that eIF3 modulates the structure of 48S complexes such that they adopt an active conformation, and may dissociate them from the IRES if this conformation is not achieved.

Cleavage was also enhanced at other internal bulged loops in the IRES on binding of 40S subunits, probably as the result of induced conformational changes. We suggest that these internal loops may act as hinges about which conformational changes can occur during assembly of 48S complexes on the IRES. We have already suggested that the pseudoknot is not rigid and may undergo structural changes on ribosome binding. A conserved A-A mispair in a helix adjacent to the pseudoknot is likely to destabilize this duplex (Kierzek et al., 1999) and may play a similar role in permitting structural transitions in the IRES during initiation. Cleavage was also enhanced at $GGC_{63–65}$ in domain II: this domain may also enhance the accuracy or stability of ribosomal binding to residues flanking the initiation codon because its deletion was found to weaken the toeprints at $UUU_{387–389}$ at the leading edge of the bound 40S subunit in binary IRES/40S subunit complexes (Fig. 7D).

MATERIALS AND METHODS

Plasmids

pCSFV(1–442)NS′ contains CSFV sequences linked to a truncated influenza NS′ reporter (Pestova et al., 1998b). PCR was used to generate mutants from it that had either a truncation of nt 1–127 or additional deletions of nt 182–234, nt 235–244, or nt 164–244. Point mutations were made in pCSFV(1–442)NS′ using a Chameleon site-directed mutagenesis kit (Stratagene, La Jolla, California). Mutations were identified by sequence analysis. The expression vectors pET(His_6-eIF4A) and its R362Q derivative have been described (Pestova et al., 1996b, 1998b).

Transcription and translation

CSFV RNAs were transcribed in vitro with T7 polymerase with or without [^{32}P]-UTP (~3,000 Ci/mmol; ICN Radiochemicals, Costa Mesa, California) from linearized plasmids (Pestova et al., 1998b). CSFV mRNAs were translated

in rabbit reticulocyte lysate (RRL; Roche Molecular Biochemicals, Indianapolis, Indiana) in the presence of [^{35}S]-methionine and with or without recombinant eIF4A (R362Q) as described (Pestova et al., 1998b; Pestova & Hellen, 1999). Translation products were resolved by electrophoresis using 12% polyacrylamide gel. Gels were exposed to X-ray film. The intensity of bands was quantitated using a Molecular Dynamics PhosphorImager.

Purification of factors and 40S ribosomal subunits

40S subunits, eIF2, and eIF3 were purified from RRL (Green Hectares, Oregon, Wisconsin) and recombinant wild-type and R362Q mutant eIF4A proteins were expressed in *Escherichia coli* and purified as described (Pestova et al., 1996a, 1996b, 1998a). The purity and quality of these factors was assessed by PAGE and using functional assays dependent on each of these factors.

Assembly and analysis of ribosomal complexes

Ribosomal complexes were assembled on 1 μg (~2.3 pmol) CSFV RNA in 40 μL reaction volumes that contained 0.4 mM GMP-PNP and [^{35}S]Met-tRNA$_i^{Met}$ (6 pmol) prepared as described (Pestova et al., 1996a), 40S subunits (6 pmol), eIF2 (16 pmol), and eIF3 (15 pmol) as indicated in the text. These ribosomal and RNP complexes were analyzed by toeprinting (Pestova et al., 1996a) using the primer 5′-CTCGTTTGCGGACATGCC-3′ (complementary to part of the NS′ sequence). cDNA products were ethanol precipitated, resuspended, and compared with appropriate dideoxynucleotide sequences by electrophoresis through 6% polyacrylamide/7 M urea gels. Ribosomal complexes were analyzed by centrifugation through a 10–30% sucrose density gradient (Pestova et al.,1996a).

Enzymatic footprinting of CSFV IRES/40S subunit complexes

Ribosomal complexes were assembled from 40S subunits and CSFV RNA in 40-μL reaction volumes essentially as described above. Free or ribosome-bound RNAs in binding buffer (20 mM Tris-HCl, pH 7.5, 2.5 mM MgAc, 100 mM KCl, 2 mM DTT) were cleaved by incubation for 10 min at 37 °C with either RNase V_1 or RNase T_1 (Amersham Pharmacia Biotech) at a final RNase V_1 concentration of 0.0007 U/μL (in the absence of 40S subunits) or of 0.00105 U/μL (in their presence) and a final RNase T_1 concentration of 0.015 U/μL (in the absence of 40S subunits) or of 0.025 U/μL (in their presence). RNAs were extracted with phenol/chloroform and precipitated with 3 vol of ethanol. The end-labeled primers 5′-CTCGTTTGCGGACATGCC-3′ (complementary to the NS′ coding sequence) or 5′-TGCAGCACCCTATCAGG-3′ (complementary to CSFV nt 309–325) were annealed to RNA and extended (Kolupaeva et al., 1996, 1998). cDNA products were analyzed by electrophoresis on 6% polyacrylamide/7 M urea gels.

ACKNOWLEDGMENTS

This work was supported by grant AI44108-01 from the National Institutes of Health.

Received March 22, 2000; returned for revision May 31, 2000; revised manuscript received August 3, 2000

REFERENCES

Brown EA, Zhang H, Ping L-H, Lemon SM. 1992. Secondary structure of the 5′ nontranslated regions of hepatitis C virus and pestivirus genomic RNAs. *Nucleic Acids Res 20*:5041–5045.

Browning KS, Leung DW, Clark SM. 1980. Protection of satellite tobacco necrosis virus ribonucleic acid by wheat germ 40S and 80S ribosomes. *Biochemistry 19*:2276–2283.

Buratti E, Tisminetzky S, Zotti M, Baralle FE. 1998. Functional analysis of the interaction between HCV 5′ UTR and putative subunits of eukaryotic translation initiation factor eIF3. *Nucleic Acids Res 26*:3179–3187.

Chon SK, Perez DR, Donis RO. 1998. Genetic analysis of the internal ribosome entry segment of bovine viral diarrhea virus. *Virology 251*:370–382.

Ehresmann C, Baudin F, Mougel M, Romby P, Ebel J-P, Ehresmann B. 1987. Probing the structure of RNAs in solution. *Nucleic Acids Res 15*:9109–9128.

Hellen CUT, Pestova TV. 1999**.** Translation of hepatitis C virus RNA. *J Viral Hepat 6*:79–88.

Honda M, Brown EA, Lemon SM. 1996. Stability of a stem-loop involving the initiator AUG controls the efficiency of internal initiation of translation on hepatitis C virus RNA. *RNA 2*:955–968.

Jackson RJ, Kaminski A. 1995. Internal initiation of translation in eukaryotes: The picornavirus paradigm and beyond. *RNA 1***:**985–1000.

Johannes G, Carter MS, Eisen MB, Brown PO, Sarnow P. 1999. Identification of eukaryotic mRNAs that are translated at reduced cap binding complex eIF4F concentrations using a cDNA microarray. *Proc Natl Acad Sci USA 96*:13118–13123.

Johannes G, Sarnow P. 1998. Cap-independent polysomal association of natural mRNAs encoding c-myc, BiP, and eIF4G conferred by internal ribosome entry sites. *RNA 4*:1500–1513.

Kamoshita N, Tsukiyama-Kohara K, Kohara K, Nomoto A. 1997. Genetic analysis of internal ribosome entry site on hepatitis C virus RNA: Implication for involvement of the highly ordered structure and cell type-specific *trans*-acting factors. *Virology 233*:9–18.

Kieft JS, Zhou K, Jubin R, Murray MG, Lau JYN, Doudna JA. 1999. The hepatitis C virus internal ribosomal entry site adopts an ion-dependent tertiary fold. *J Mol Biol 292*:513–529.

Kierzek R, Burkard ME, Turner DH. 1999. Thermodynamics of single mismatches in RNA duplexes. *Biochemistry 38*:14214–14223.

Kolk MH, Van der Graaf M, Wijmenga SS, Pleij CWJ, Heus HA, Hilbers CW. 1998. NMR structure of a classical pseudoknot: Interplay of single- and double-stranded RNA. *Science 280*:434–437.

Kolupaeva VG, Hellen CUT, Shatsky IN. 1996. Structural analysis of the interaction of the pyrimidine tract-binding protein with the internal ribosomal entry site of encephalomyocarditis virus and foot-and-mouth disease virus RNAs. *RNA 2*:1199–1212.

Kolupaeva VG, Pestova TV, Hellen CUT. 2000. An enzymatic footprinting analysis of the interaction of 40S ribosomal subunits with the internal ribosomal entry site of hepatitis C virus. *J Virol 74*:6242–6250.

Kolupaeva VG, Pestova TV, Hellen CUT, Shatsky IN. 1998. Translation initiation factor eIF4G recognizes a specific structural element within the internal ribosomal entry site of encephalomyocarditis virus RNA. *J Biol Chem 273*:18599–18604.

Kozak M. 1977. Nucleotide sequences of 5′-terminal ribosome-protected initiation regions from two reovirus messages. *Nature 269*:390–394.

Kozak M, Shatkin AJ. 1977. Sequences and properties of two ribosome binding sites from the small size class of reovirus messenger mRNA. *J Biol Chem 252*:6895–6908.

Le SY, Liu WM, Maizel JV. 1998. Phylogenetic evidence for the im-

proved RNA higher-order structure in internal ribosome entry sequences of HCV and pestiviruses. *Virus Genes 17*:279–295.
Legon S. 1976. Characterization of the ribosome-protected regions of I^{125}-labelled rabbit globin messenger RNA. *J Mol Biol 106*:37–53.
Lemon SM, Honda H. 1997. Internal ribosome entry sites within the RNA genomes of hepatitis C virus and other flaviviruses. *Semin Virol 8*:274–288.
Merrick WC. 1992. Mechanism and regulation of eukaryotic protein synthesis. *Microbiol Rev 56*:291–315.
Odreman-Macchioli FE, Tisminetzky SG, Zotti M, Baralle FE, Burotti E. 2000. Influence of correct secondary and tertiary RNA folding on the binding of cellular factors to the HCV IRES. *Nucleic Acids Res 28*:875–885.
Pause A, Méthot N, Svitkin Y, Merrick WC, Sonenberg N. 1994. Dominant negative mutants of mammalian translation initiation factor eIF-4A define a critical role for eIF-4F in cap-dependent and cap-independent initiation of translation. *EMBO J 13*:1205–1215.
Pelletier J, Flynn ME, Kaplan G, Racaniello V, Sonenberg N. 1988. Mutational analysis of upstream AUG codons of poliovirus RNA. *J Virol 62*:4486–4492.
Pestova TV, Borukhov SI, Hellen CUT. 1998a. Eukaryotic ribosomes require eIFs 1 and 1A to locate initiation codons. *Nature 394*:854–859.
Pestova TV, Hellen CUT. 1999. Internal initiation of translation of bovine viral diarrhea virus RNA. *Virology 258*:249–256.
Pestova TV, Hellen CUT, Shatsky IN. 1996a. Canonical eukaryotic initiation factors determine initiation of translation by internal ribosomal entry. *Mol Cell Biol 16*:6859–6869.
Pestova TV, Lomakin IB, Lee JH, Choi SK, Dever TE, Hellen CUT. 1999. The ribosomal subunit joining reaction in eukaryotes requires eIF5B. *Nature 403*:332–335.
Pestova TV, Shatsky IN, Fletcher SP, Jackson RJ, Hellen CUT. 1998b. A prokaryotic-like mode of cytoplasmic eukaryotic ribosome binding to the initiation codon during internal initiation of translation of Hepatitis C virus and Classical swine fever virus RNAs. *Genes & Dev 12*:67–83.
Pestova TV, Shatsky IN, Hellen CUT. 1996b. Functional dissection of eukaryotic initiation factor 4F: The 4A subunit and the central domain of the 4G subunit are sufficient to mediate internal entry of 43S preinitiation complexes. *Mol Cell Biol 16*:6870–6878.
Pilipenko EV, Pestova TV, Kolupaeva VG, Khitrina EV, Poperechnaya AN, Agol VI, Hellen CUT. 2000. A cell-cycle-dependent protein serves as a template-specific translation initiation factor. *Genes & Dev 14*:2028–2045.
Psaridi L, Georgopoulou U, Varaklioti A, Mavromara P. 1999. Mutational analysis of a conserved tetraloop in the 5′ untranslated region of hepatitis C virus identifies a novel RNA element essential for the internal ribosome entry site function. *FEBS Lett 453*:49–53.
Reynolds JE, Kaminski A, Carroll AR, Clarke BE, Rowlands DJ, Jackson RJ. 1996. Internal initiation of translation of hepatitis C virus RNA: The ribosome entry site is at the authentic initiation codon. *RNA 2*:867–878.
Reynolds JE, Kaminski A, Kettinen H-J, Carroll AR, Rowlands DJ, Jackson RJ. 1995. Unique features of internal initiation on hepatitis C virus. *EMBO J 14*:6010–6020.
Rijnbrand RC, Abbink TE, Haasnoot PC, Spaan WJ, Bredenbeek PJ. 1996. The influence of AUG codons in the hepatitis C virus 5′ nontranslated region on translation and mapping of the translation initiation window. *Virology 226*:47–56.
Rijnbrand R, van der Straaten T, van Rijn PA, Spaan WJ, Bredenbeek PJ. 1997. Internal entry of ribosomes is directed by the 5′ noncoding region of classical swine fever virus and is dependent on the presence of an RNA pseudoknot upstream of the initiation codon. *J Virol 71*:451–457.
Shine J, Dalgarno L. 1974. The 3′-terminal sequence of *Escherichia coli* 16S ribosomal RNA: Complementarity to nonsense triplets and ribosome binding sites. *Proc Natl Acad Sci USA 71*:1342–1346.
Sizova DV, Kolupaeva VG, Pestova TV, Shatsky IN, Hellen CUT. 1998. Specific interaction of eukaryotic translation initiation factor 3 with the 5′ nontranslated regions of hepatitis C virus and classical swine fever virus RNAs. *J Virol 72*:4775–4782.
Sundkvist IC, Staehelin T. 1975. Structure and function of free 40S ribosome subunits: Characterization of initiation factors. *J Mol Biol 99*:401–418.
Tsukiyama-Kohara K, Iizuka N, Kohara M, Nomoto A. 1992. Internal ribosomal entry site within hepatitis C virus RNA. *J Virol 66*:1476–1483.
Wang C, Le S, Ali N, Siddiqui A. 1995. An RNA pseudoknot is an essential structural element of the internal ribosome entry site located within the hepatitis C virus 5′ noncoding region. *RNA 1*:526–537.
Wang C, Sarnow P, Siddiqui A. 1994. A conserved helical element is essential for internal initiation of translation of hepatitis C virus RNA. *J Virol 68*:7301–7307.
Wilson JE, Pestova TV, Hellen CUT, Sarnow P. 2000. Initiation of protein synthesis from the A-site of the ribosome. *Cell 102*:511–520.